Silicon Mechanical Sensors for High-Temperature Control Systems. *Principles of Monolithic IPT Modeling for the 0÷300 °C Temperature Range.*

Michael Tikhomirov
1989

Abstract

This chapter presents principles for modeling monolithic integrated piezoresistor transducers (IPTs) in silicon mechanical sensors for automatic control systems operating in the 0–300°C temperature range. The upper operational limit is determined by the insulating resistance of p-n junctions reaching a critical value, affecting the bridge circuit's transfer coefficient. Analytical expressions for reverse current density and temperature dependencies are derived, considering factors like charge carrier mobility, lifetime, and diffusion length. A symmetric four-branch bridge circuit topology is proposed, minimizing p-n junction area (≤2×10⁻⁴ cm²) and temperature errors through optimized piezoresistive channel dimensions and doping.

For IPTs with distributed parameters (channel conductivity 2–10 times that of the elastic element at ρ_ee ≤20 Ω·cm), a discrete analog model using Bessel functions accounts for current redistribution, yielding equations for gauge factor and input resistance. Experimental validation on beam force IPTs fabricated from n-type silicon (ρ_ee=4.5 Ω·cm) with boron ion implantation shows the upper limit at 180–200°C, with discrepancies from calculations ≤15%. Results enable extension of the temperature range to ≥210°C for low-resistivity elements, supporting miniaturized, high-precision sensors in harsh environments.

The upper limit of the operating temperature range, denoted as T_{max}, for a monolithic IPT with an insulating $p-n$ junction, is determined by the conditions under which the insulating resistance R_i^{p-n} of the junction reaches a critical value $R_{i_{\min}}^{p-n}$. At $R_{i_{\min}}^{p-n}$, the resistance shunt effect EE on one of the MC arms alters the value of the transfer coefficient K_{mc} by $1.\%$ relative to the nominal value, which is equal to $K_{mc} = 10\ \frac{mV}{V}$.

From [1], where an IPT with a resistance PCH equivalent to $R_{ch} = 1000\ \Omega$ was examined, the upper limit of the range corresponds to a temperature $T_{max} = T_{per}$ when the junction of the reverse bias voltage $p-n$ of $U_{rev} = 5\ V$ has a reverse current VA of $I_{rev} = 2 \cdot 10^{-6}\ A$. For this particular IPT design, it is assumed that within the temperature range $T_{min} \leqslant T \leqslant T_{max}$, MC have lumped parameters, and the physical principle of converting mechanical matter into an electrical signal is both studied and considered to be indisputably true.

Therefore, modeling and experimental studies are mainly concerned with the analysis of temperature dependencies in the range of $(0 \div 300)^{\circ}C$ for the parameter VAC of the isolating $p-n$ junction, which determines R_i^{p-n}, the reverse current density $J_{rev}(T)$.

In the context of IPT without insulating $p-n$ junctions, where the MC with distributed parameters PCH exhibit conductivity 1 to 10 times higher than EE conductivity, it should be noted that the physical principle of conversion has not been thoroughly explored. This situation requires modeling and experimental procedures to determine the upper operating temperature limit and to examine the changes in the parameters of IPT as the resistance values EE change at $\rho_{ee} \leqslant 20\ \Omega \cdot cm$ within the temperature range of $(0 \div 350)^{\circ}C$.

To improve the precision of experimental studies and simplify the modeling of miniature monolithic IPT with an extended operational temperature range up to $300^{\circ}C$, it is essential to define their inherent design solutions. In domestic practice, the highest precision of geometric dimensions is achieved for monolithic structures IPT of weakly and medium-alloyed silicon wafers with orientation in the plane (001) chemical profiling method [2]. This anisotropic etching method can be used for most EE types in use, and in such IPT tensometric channels doped with an acceptor impurity are arranged parallel and perpendicular to the elastic element's boundaries along the species directions [110]. This results in proportional changes in resistances at small deformations, which are close in magnitude and opposite in sign [3].

The design of the deformation transducer that satisfies the aforementioned requirements includes identical square contact pads MC with a size of b. The centers of these pads are located at the vertices of a square with a

size of a. These pads are interconnected by four single bands PCH with a width of d_{ch}. These include both longitudinal ($R_{1,3}$) and transverse ($R_{2,4}$) piezoresistors.

These contact pads and piezoresistive channels are created by local doping, specifically boron doping, of the planar surface of the oriented monolithic monocrystalline silicon structure (001) $BR-EE$. The elements MC are positioned in the body EE with a thickness of H_{ee}, distanced C from the basal border H_w.

The above design considerations ensure the minimization of the temperature gradient in the placement plane PCH within EE, the equality of all thermal resistances in the heat sink chain $PCH-EE-BR$, and the reduction of the values and variances of initial deformations in the placement areas PCH. Furthermore, they ensure the minimization of deviations in the electrical resistance IPT from the average values and the uniformity of their temperature characteristics. This results in a reduction of the complementary temperature error IPT and brings the value and temperature dependence of the normalized null output K_{mc0} closer to zero.

Assuming $K_0(T)=0$, the transformation characteristic for any mechanical

$$\frac{V_{\text{out}}}{V_{\text{in}}}=K_{mc}\cdot K_{ch}\cdot\varepsilon= \\ =2\cdot K_{\parallel}\cdot\varepsilon_{x_0}\cdot\left[\frac{1-\frac{K_{\perp}}{K_{\parallel}}\frac{(\varepsilon_{x_4}+\varepsilon_{x_2})}{2\varepsilon_{x_0}}}{\left[2+K_{\parallel}\cdot\varepsilon_{x_0}\cdot\left(1+\frac{K_{\perp}}{K_{\parallel}}\cdot\frac{\varepsilon_{x_2}}{\varepsilon_{x_0}}\right)\right]\cdot\left[2+K_{\parallel}\cdot\varepsilon_{x_0}\cdot\left(1+\frac{K_{\perp}}{K_{\parallel}}\cdot\frac{\varepsilon_{x_4}}{\varepsilon_{x_0}}\right)\right]}\right] \quad (36)$$

where $K_{\parallel}, K_{\perp}$ are the longitudinal and transverse gauge factor of the silicon channel PCH, respectively; ε_{x_0} is the amount of strain EE at the geometric centers of piezoresistors $R_1; R_3$ channels; $\varepsilon_{x_2}, \varepsilon_{x_4}$ - deformation values in the geometric centers of piezoresistors $R_2; R_4$ channels.

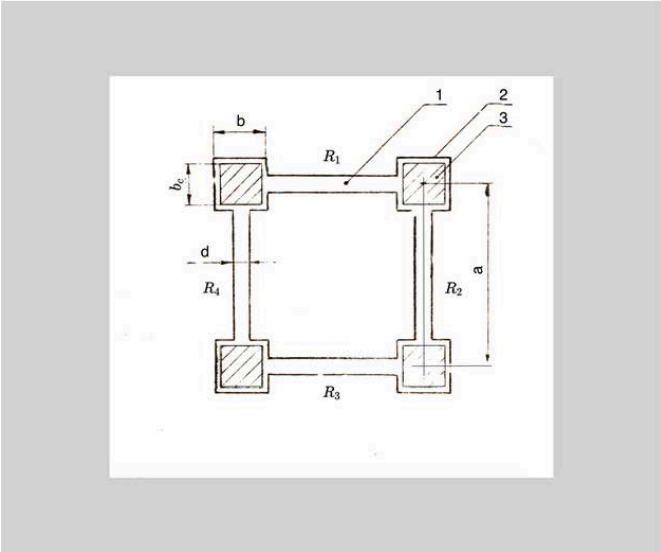

Firure 12. Topological structure of a symmetric four-branch bridge circuit. 1-piezoresistive channel; 2-diffusion contact pad of p-type; 3-contact "Al-Si (p-type)".

For the selected MC, the total area A_{p-n} and perimeter P_{p-n} of the insulating p-n junction are determined by the relations:

$$A_{p-n}=4\left[b^2+d_{ch}(a-b)\right]; \quad (37)$$

$$P_{p-n}=8[a+b-d_{ch}] \quad (38)$$

The standard value of R_{in} for piezoresistive mechanical sensors is in the range $(95\div1520)\ \Omega$ [4]. In this case, at $d_{ch}=1\cdot10^{-3}\ cm$ and the surface resistance of the ion alloy layer equal to $85\ \Omega/\square$, the channel length $(a-b)$ is within $(10\div200)\cdot10^{-4}\ cm$ and the total junction area $p-n$ at $b=40\cdot10^{-4}\ cm$, is $A_{p-n}=(0.5\div2)\cdot10^{-4}\ cm^2$. MC with such miniature dimensions can be composed of a small diaphragm, beam, and other elastic elements in mechanical IPT. When the size of the elastically deformable part EE is greater than $0.2\ cm\times0.2\ cm$, we can assume that the equality $\varepsilon_{x_2}\approx\varepsilon_{x_4}\approx\varepsilon_{x_0}$ holds, then for IPT, where $|K_{\parallel}|\approx|K_{\perp}|$, from (36) the transformation characteristic will be:

$$\frac{V_{out}}{V_{in}} = 0.5 \cdot K_{\parallel} \cdot \varepsilon_{x_0} \left(1 - \frac{K_{\perp}}{K_{\parallel}}\right). \qquad (39)$$

1. Monolithic IPTs with Isolating P-N Junction

In deriving the calculated dependence of the inverse current density J_{rev} on temperature to determine the upper limit of the operating temperature range of monolithic IPT, where PCH p-type in EE n-type are isolated by a layer of carrier-poor $p-n$ junction , the following conditions, initial data and calculation relations were chosen.

(1) The dependence of $I_{rev}(T)$ is determined by relations (21)-(25) and temperature changes of parameters:

- of free charge carriers $n_i(T)$ from relation (25);
- the lifetime $\tau_p(T)$ for the minority charge carriers in the body EE from the graph in Fig. 2.9;
- the lifetime of $\mu_p(T)$ for the minority charge carriers in the EE body from the relation [5] :

$$\mu_p(T) = \mu_{p0}\left(\frac{T_0}{T}\right)^{2.5} \qquad (40)$$

  where $\mu_{p0}(T)$ is the hole mobilitat temperature $T_0 = 293\ K$;
- the diffusion length $L_p(T)$ for the minority charge carriers in the body EE from the relation:

$$L_p(T) = \left(\frac{\mu_p(T) \cdot \tau_p(T) \cdot k \cdot T}{q}\right)^{1/2} \qquad (41)$$

- S_0 – does not change with temperature and is equal to the maximum value $S_0 = 1 \cdot 10^4$ cm/sec.

(2) $P-N$ junction is a sharp, asymmetric, stepped, $p-n$ type junction (that is, $\tilde{\rho}_{ch} \ll \rho_{ee}$) with the width of the bulk charge region in the EE body equal to

$$d_{p-n} \approx 3.65 \cdot 10^3 \left(\frac{(V_{rev})}{N_e^{EE}}\right)^{1/2} \qquad (42)$$

a uniform distribution of bulk charges along the metallurgical junction boundary.

(3) In the topological structure MC in Fig. 3.1, the geometric parameter b is given a constant value equal to $b = 40 \cdot 10^{-4}\ cm$. For the calculations, $b = d_{ch}$, then changing the area of the insulating p-n junction is possible only by changing the length of PCH $l_{ch} = (a - b)$. The ratio of the perimeter $p-n$ junction P_{p-n} to the area A_{p-n} is a constant value equal to

$$K_{p-n} = \frac{P_{p-n}}{A_{p-n}} = 500\ cm^{-1} \qquad (43)$$

(4) The reverse bias voltage $p-n$ junction and supply voltage MC are $V_{rev} = V_{in} = 5V$.

(5) The boundary values of the resistances EE are determined by the values:
$\rho_{ee1} = 20\ \Omega \cdot cm$, from the graph in Fig.9 the intrinsic conductivity temperature $+150^{\circ}C$;$\rho_{ee1} = 0.5\ \Omega \cdot cm$ is the calculated value of the breakdown voltage $p-n$ transition in the EE volume, chosen equal to $V_{br} = 10 \cdot V_{in}$ from the ratio:

$$V_{br} = 10 \cdot V_{in} = 86 \cdot \rho_{ee} \qquad (44)$$

$\rho_{ee1} = 4.5\ \Omega \cdot cm$ is the standard resistivity value of silicon wafers in IPT production.

(6) Initial temperature value $T_0 = 293K$.

Taking into account the selected initial data and the calculated relations, the temperature dependence of the reverse current density VAC of the IPT isolating $p-n$-junction is determined by the following expression:

$$J_{rev} = q \cdot a_{p-n} \cdot \left(\frac{1}{\tau_p(T)} + S_0 \cdot K_{p-n}\right) \cdot e^{22.2 \cdot \left(\frac{T-293}{T}\right)} + \\ + q \cdot \left[\left(\frac{k \cdot \mu_{p0}}{q \cdot \tau_p(T)}\right)^{1/2} \cdot \left(\frac{113.7}{T}\right)^3 \cdot P_n \cdot e^{22.2 \cdot \left(\frac{T-293}{T}\right)}\right] \cdot e^{22.2 \cdot \left(\frac{T-293}{T}\right)} \qquad (45)$$

where $a_{p-n} = \frac{d_{p-n} \cdot n_{i0}}{2}$ is a parameter characterizing the concentration of intrinsic charge carriers n_{i0} in the $p-n$ junction region at temperature $T = 293\ K$; $P_n = \frac{n_{i0}^2}{N_0^{ee}}$ is the concentration of minority charge carriers in the EE body at $T = 293\ K$; $k = 1.38 \cdot 10^{-23}$ J/K - Boltzmann constant.

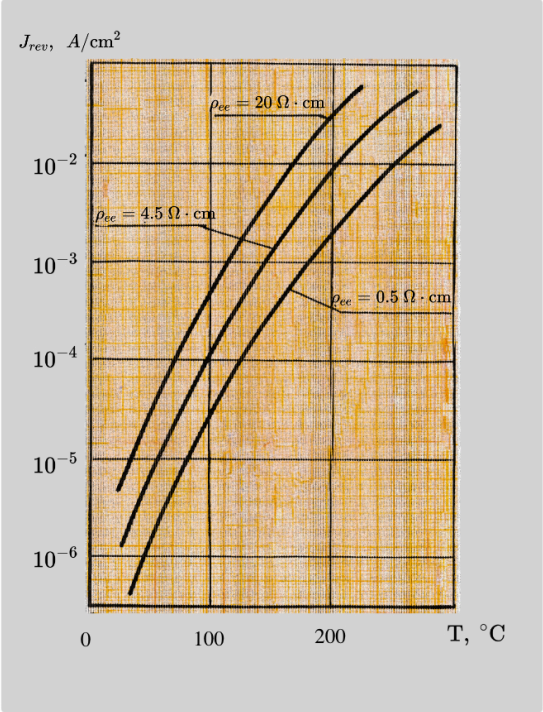

Figure 13. Calculated dependences of reverse current density J_{rev} of p-n junction IPT on temperature for different values of resistivity of elastic element ρ_{ee}

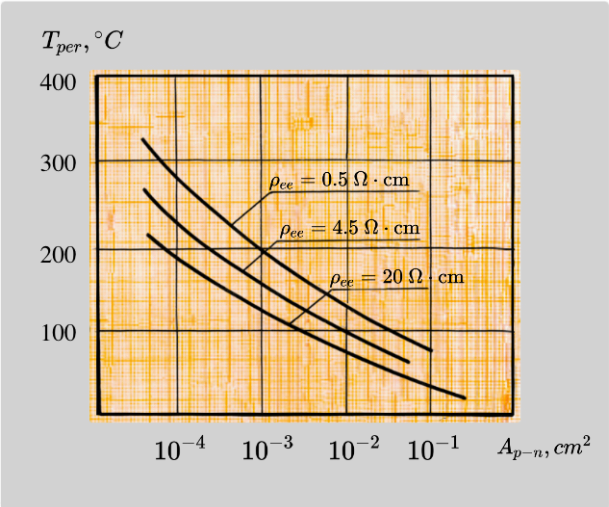

Figure 14. Calculated dependences of permissible temperature T_{per} values on the area of insulating p-n junction A_{p-n} for different values of resistivity of elastic element ρ_{ee}

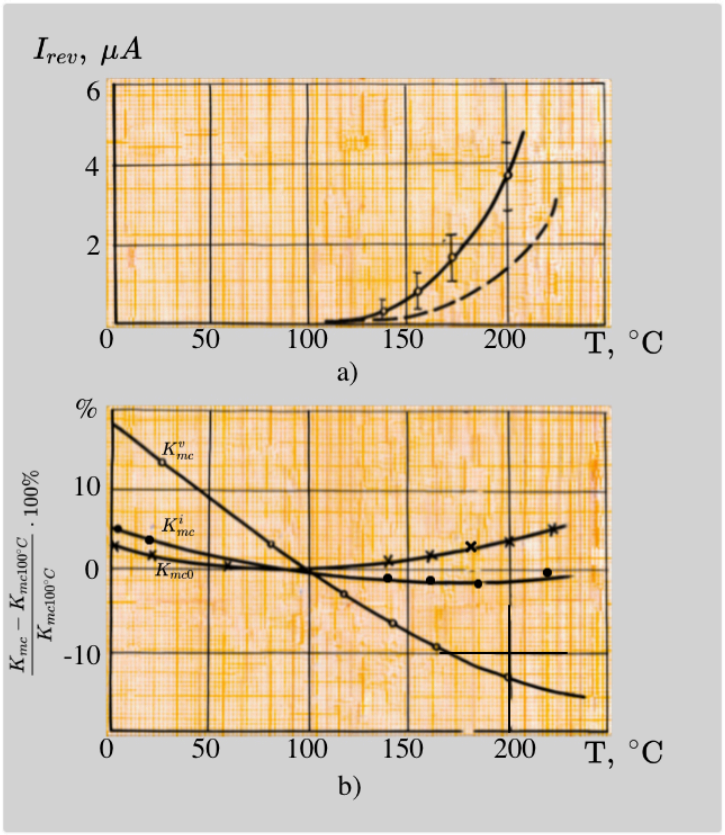

Figure 15. Temperature dependences of IPT sample parameters: a) I_{rev} reverse current: —— experimentally, - - - calculated ; b) K_{mc0} - initial transfer coefficient, K^v_{mc} - IPT transfer coefficient when $V_{in} = 5$ V stabilized voltage is fed to the MC, K^i_{mc} - IPT transfer coefficient when $I_{in} = 5\mu A$ stabilized current is fed to the MC

Fig. 3.2 shows the calculated dependences of $J_{rev}(T)$ for the selected values of ρ_{ee} on which the dependences of the allowable temperature values T_{per} on the area of the insulating junction $p-n$ are plotted in Fig. 3.3. For the chosen topological structure, the minimum allowable value A^{min}_{p-n} can be determined by the minimum standard value of the piezoresistor resistance equal to 95 Ω and the surface resistance of the piezoresistive layer equal to the ion-alloy layers $(80 \div 150)\ \Omega/\square$. In this case, the geometric parameter $\frac{a-b}{b} \approx 1$ and the area $A^{min}_{p-n} = 1.28 \cdot 10^{-4}\ cm^2$. From the graphs in Fig. 3.3, the upper limit of the operating temperature range for A^{min}_{p-n} is determined by the values $185°C$, $225°C$ and $275°C$ at resistances of the elastic element of $20\ \Omega \cdot cm$, $4.5\ \Omega \cdot cm$ and $0.5\ \Omega \cdot cm$, respectively.

To experimentally verify the calculations, the beam forces IPT were fabricated from single-crystal silicon n type with orientation (001) and resistivity $\rho_{ee} = 4.5\ \Omega \cdot cm$. The geometric parameters of the topological structure are as follows: $b = 40 \cdot 10^{-4}\ cm$; $b = d$; $a = 3 \cdot b$, $A_{p-n} = 1.92 \cdot 10^{-4}\ cm^2$; $K_{p-n} = \frac{P_{p-n}}{A_{p-n}} = 500\ cm^{-1}$. PCH were formed by boron ion implantation technology with a doping dose of $2 \cdot 10^{15}\ cm^{-2}$. The surface resistivity of the piezoresistive layers doped with ions $R_s = 85\ \Omega/\square$.

Fig. 3.4 shows experimental for IPT samples and calculated from the graph in Fig. 3.2 for this topological structure MC dependences of the reverse current I_{rev} VAC on temperature, by which the upper limit of the temperature range (value T_{per} at $I_{rev} = 2\ \mu A$) is determined:

- for samples IPT values $+180°C \div +200°C$

- for the value $+210^{\circ}C$ calculated from formula (45).

The experimentally measured temperature dependences $K_{mc0}(T)$, $K^{u}_{mc}(T)$, and $K^{i}_{mc}(T)$ in Fig. 3.4(b) are characterized by smooth changes throughout the range up to the limit temperature of the research $+260^{\circ}C$.

The calculations performed and experimental studies give grounds to assert that monolithic silicon integral piezoresistive transducers with the isolation of piezoresistive channels of p-type conductivity from EE by the $p-n$ junction layer are able to work up to temperatures $+180^{\circ}C \div 300^{\circ}C$. The specific limits of the operating range will be determined by the values of the resistivity and geometrical parameters of the topological structure MC selected during the design.

2. Monolithic IPT with Distributed Parameters

The physical meaning of the modeling and research was to find the relations between the electrophysical characteristics of EE and PCH, allowing to calculate and design IPT extended beyond the critical temperature $T_{per} = 150^{\circ}C$=150 C, operating range, provided that the conductivity $(2 \div 10)$ is times the conductivity of EE, that is, at $\rho_{ee} < 20\ \Omega \cdot cm$.

The determination of computational relationships is related to the problem of building and investigating the MC model with distributed parameters PCH, which are formed in the volume of an equal-thick silicon wafer.

For the modeling, the strain transducer design shown in Fig. 3.1 and Fig. 3.5, consisting of a silicon elastic element 1 p-type with orientation in the plane (100) and thickness H_{ee}, in which equal square contact pads 8, 9,10, 11 with sides b with centers at the vertices of a square with sides $(a+b)$, are connected by four single-band piezoresistive channels p^{+}-type 2,3,4,5 oriented along crystallographic directions $[011]$ with width equal to b and thickness - x_j .

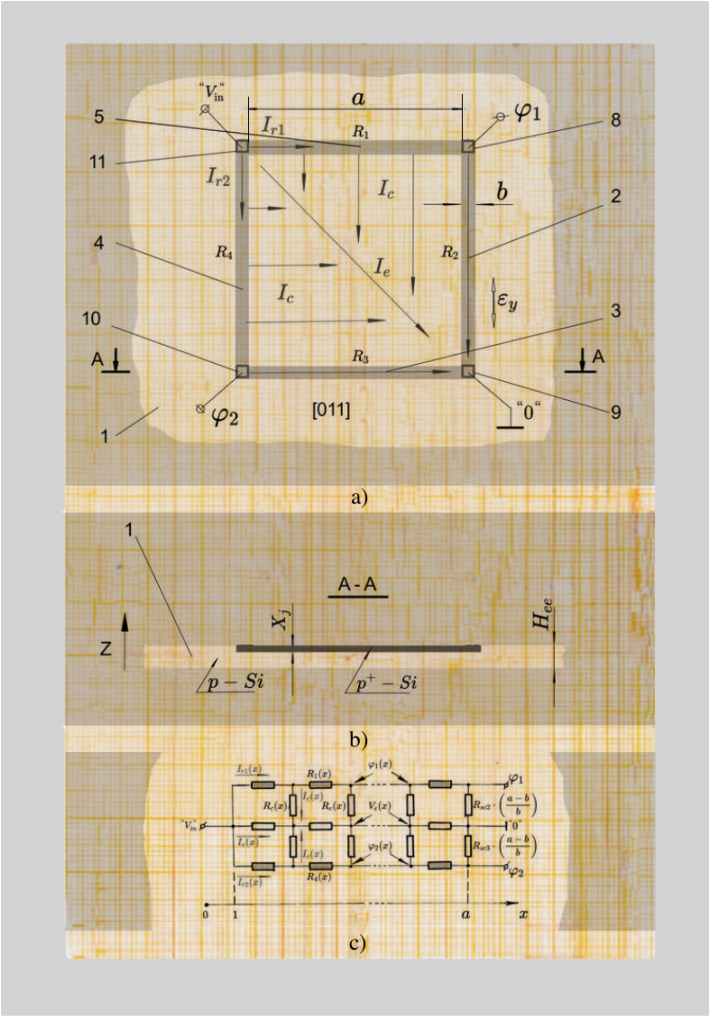

Figure 16. Deformation transducer along the X-axis, selected for modeling the characteristics of the transducer with distributed parameters: a) - topological structure of the IPT; b) - also, second projection, section along A - A; c) - equivalent diagram of the analog of the discrete model.

The problem is solved under the following conditions and assumptions:

- - $a \gg H_{ee}$;
- the strain component ε_y is directed along the crystallographic trajectory [011];
- the bridge circuit is fed from the stabilized voltage source V_{in} through the diagonal contacts 9,11;
- current I_r is evenly distributed with respect to the plane of cross section of channels 2,3,4,5; its distribution is similar in neighboring channels 2,3 and 4,5 with common contacts 11,9, respectively;
- the current in the elastic element 1 is evenly distributed in the cross section in the direction Z along the normal to the flat surface of the elastic element 1; currents are absent outside the circuit area bounded by channels 2,3,4,5; inside the area are characterized by components I_c and I_e; the direction of components I_c is normal relative to the sides of neighboring channels 4,5 with a common power contact 11; current component I_e is directed along the diagonal connecting power contacts 9,11;
- distribution of concentration of majority carriers in the channels 2,3,4,5 is uniform; the level of doping is characterized by the value of resistivity equal to the mean value of resistivity at real non-uniform distribution of impurity; $R_{Sc} = \frac{\tilde{\rho}_{ch}}{x_j}$ where R_{Sc} - values of surface resistance of channels 2,3,4,5 , $\Omega/\square$; x_j - doping depth of channels 2,3,4,5, cm, equal to depth of p-n junction, if elastic element 1 of silicon n-type;
- the level of doping of elastic element 1 is characterized by the value of resistivity of the initial material ρ_{ee}.

As a discrete analogue of the transducer model, we used the equivalent circuit of a long line with parameters distributed along the X axis, shown in Fig. 3.5. c), for which the differential equations linking currents and

potentials have the form:

$$\begin{cases} I_{r1}(x) = -\frac{d\varphi_1(x)}{dx} \cdot \frac{b}{R_{Sc1}}; \\ I_{r2}(x) = -\frac{d\varphi_2(x)}{dx} \cdot \frac{b}{R_{Sc4}}; \end{cases} \begin{cases} I_c(x) = -\frac{dI_{r1}(x)}{dx}; \\ I_c(x) = -\frac{dI_{r2}(x)}{dx}; \end{cases} \\ I_e(x) = -\frac{dV_{in}(x)}{dx} \cdot \frac{b \cdot H_{ee}}{\sqrt{2} \cdot \rho_{ee}}; \quad \frac{dI_e(x)}{dx} = 2I_c(x). \end{cases} \tag{46}$$

After transformations (46), the differential equations look like

$$\begin{cases} \frac{d^2\Upsilon_1(x)}{dx^2} = x^{-1}C_1 \cdot \Upsilon_1(x); \\ \frac{d^2\Upsilon_2(x)}{dx^2} = x^{-1}C_2 \cdot \Upsilon_2(x), \end{cases} \tag{47}$$

where

$$\Upsilon_1(x) = \varphi_1(x) - V_{in}(x);$$
$$\Upsilon_2(x) = \varphi_2(x) - V_{in}(x);$$
$$C_1 = \left(2\sqrt{2} + \frac{R_{Sc1}}{\rho_{ee}} H_{ee}\right);$$
$$C_2 = \left(2\sqrt{2} + \frac{R_{Sc4}}{\rho_{ee}} H_{ee}\right).$$

The solution of equations (47) has the form [6]:

$$\Upsilon(x) = \sqrt{x} Z_1(i \cdot 2\sqrt{Cx}) \tag{48}$$

where $Z_1(i \cdot 2\sqrt{Cx})$ is a Bessel function with an imaginary unit.
The following boundary conditions were used:
at $x = 1 : \Upsilon_1(1) = \Upsilon_2(1) = 0;\ \varphi_1(1) = \varphi_2(1) = V_{in};$
$V_{in}(1) = V_{in}$;
at $x = a :\ \Upsilon_1(a) = \varphi_1;\ \Upsilon_2(a) = \varphi_2;\ V_{in}(a) = 0;$
$\varphi_1(a) = \varphi_1;\ \varphi_2(a) = \varphi_2;$
$I_{r_1}(a) = \varphi_1 \frac{b}{R_{Sc2} \cdot a};\ I_{r_2}(a) = \varphi_2 \frac{b}{R_{Sc3} \cdot a};$
$I_{in} = I_e(a) + 2I_c(a);\ I_e(a) = I_{in} - \varphi_1 \frac{b}{R_{Sc2} \cdot a} - \varphi_2 \frac{b}{R_{Sc3} \cdot a};$
with which, the solution of equations (47) determined the following relations for circuit parameters:

$$V_{out}^{dp} = \varphi_1 - \varphi_2 =$$
$$= V_{\text{in}} \cdot \left(\frac{R_2}{R_1 + R_2 + \frac{R_1 \cdot R_2 \cdot b}{\rho_{ee} \cdot a} H_{ee} \cdot \Phi} - \frac{R_3}{R_4 + R_3 + \frac{R_3 \cdot R_4 \cdot b}{\rho_{ee} \cdot a} H_{ee} \cdot \Phi} \right); \tag{49}$$

$$R_{in}^{dp} = \left[\frac{1 + 2\frac{R_2 \cdot b}{\rho_{ee} \cdot a} H_{ee} \cdot \Phi}{R_1 + R_2 + \frac{R_1 \cdot R_2 \cdot b}{\rho_{ee} \cdot a} H_{ee} \cdot \Phi} + \frac{1}{R_3 + R_4 + \frac{R_3 \cdot R_4 \cdot b}{\rho_{ee} \cdot a} H_{ee} \cdot \Phi} + \frac{b \cdot H_{ee}}{\rho_{ee} \cdot a\sqrt{2}} \right]^{-1}; \tag{50}$$

where V_{out} is the value of the output of the bridge circuit, V; R_{in} - value of input resistance of the bridge circuit, Ω; R_1, R_2, R_3, R_4 - resistance values of piezoresistive channels 5,4,3,2 electrically isolated from each other in the four shoulders of the bridge circuit, Ω; Φ is a dimensionless coefficient for the strain transducer model, which characterizes the redistribution of the charge carrier current in the channels and the elastic element.

We assume that

$$R_1 = R_2 = R_3 = R_4 = R_{ch} = \tilde{\rho}_{ch} \cdot \frac{a}{b \cdot x_j}; \\ \frac{dR_2}{d\varepsilon_x} = -\frac{dR_1}{d\varepsilon_x} = \frac{dR_4}{d\varepsilon_x} = -\frac{dR_3}{d\varepsilon_x} = R_{ch} \cdot K_{ch}; \tag{51}$$

where K_{ch} is the gauge factor of electrically isolated piezoresistive channels 2,3,4,5. Then the transducer gauge factor and the input resistance of the bridge circuit are equal:

$$K_{mc}^{dp}(T, \varepsilon_y) = \frac{1}{V_{in}} \frac{dV_{out}}{d\varepsilon_y} = \frac{2K_{ch}(T)}{2 + \frac{\tilde{\rho}_{ch}(T)}{\rho_{ee}(T)} \cdot \frac{H_{ee} \cdot \Phi}{x_j}}; \tag{52}$$

$$R_{in}^{dp}(T) = 0.5 \cdot R_{ch}(T) \left[\frac{1 + \frac{R_{ch}(T)}{\rho_{ee}(T)} \cdot \frac{H_{ee} \cdot \Phi \cdot b}{a}}{2 + \frac{R_{ch}(T)}{\rho_{ee}(T)} \cdot \frac{H_{ee} \cdot \Phi \cdot b}{a}} + 0.354 \frac{R_{ch}(T) \cdot H_{ee} \cdot b}{\rho_{ee}(T) \cdot a} \right]^{-1} \quad (53)$$

where $K_{ch}(T) = K_0 + K_1 \frac{T_0}{T} + K_2 \left(\frac{T_0}{T} \right)^2$ is the gauge factor of electrically isolated piezoresistive channels 2,3,4,5 with temperature dependence determined according to [7] by second degree polynomial in case the temperature parameter t, $t = \frac{T_0}{T}$. This is true for silicon piezoresistors [8]; $\alpha_{ch}[1/K], \beta_{ch}\left[1/K^2\right]$ are approximation coefficients; $\tilde{\rho}_{ch0}$ - is the resistivity at $T = T_0$;

$$R_{ch}(T) = \rho_{ch}(T) \cdot \frac{a}{b \cdot x_j} = R_{ch0} \left[1 + \alpha_{ch} (T - T_0) + \beta_{ch} (T - T_0)^2 \right]$$

- resistance value of electrically isolated piezoresistive channels 2,3,4,5; R_{ch0} - is the resistance at $T = T_0$; $\rho_{ee}(T) = \rho_{ee0} \left[1 + \alpha_{ee} (T - T_0) + \beta_{ee} (T - T_0)^2 \right]$ - is the resistivity of the initial silicon wafer 7 with the temperature dependence defined by the polynomial of the second degree; $\alpha_{ee}[1/K], \beta_{ee}\left[1/K^2\right]$ are approximation coefficients.

For any transducer design, the condition $a \leq H_{ee}$ is possible. Then the assumptions about the uniformity of the current distribution in the elastic element along the direction Z will not be adequate to the nature of the distribution in the real object. Therefore, instead of H_{ee}, its effective value H_{ef} is used. The redistribution parameter of the current of charge carriers in the channels and the elastic element in this case is equal to:

$$\Lambda = \frac{H_{ef} \cdot \Phi \cdot b}{a}. \quad (54)$$

The numerical value of the parameter Λ is determined by joint measurements [9]. With known values of the temperatures within the selected operating range T_1 and T_2, the values R_{inT1} and R_{inT2} are measured. For the same temperature values, the values R_{chT1} , R_{chT2} are calculated. If α_{ch} and β_{ch} are unknown a priori, R_{chT1} and R_{chT2} are measured on specially designed test samples. The same is true for ρ_{eeT1} and ρ_{eeT2}. Using the system of 2 equations derived from (53), we obtain the ratio to calculate Λ.

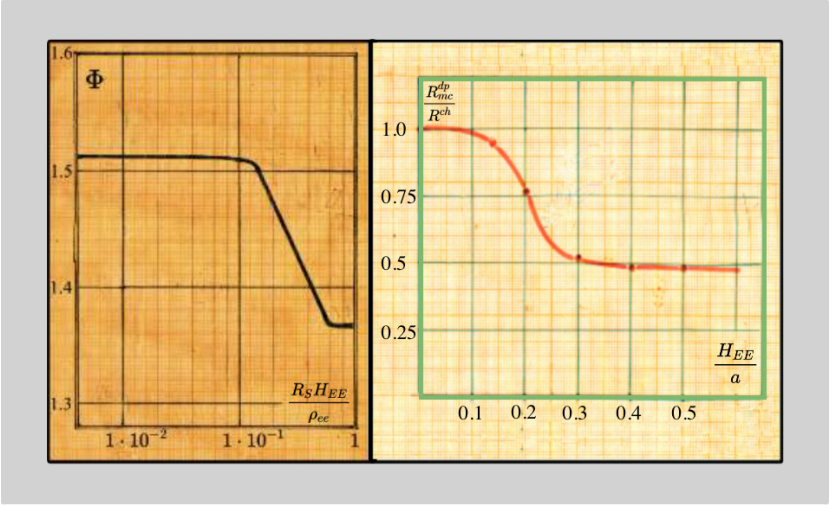

Figure 17. Experimentally obtained dependences of the change in the coefficient Φ and the input resistance R_{mc}^{dp} on the design parameters for IPT with distributed parameters.

The test IPT was made of silicon wafers of KDB-0.5, KDB-1 and KDB-10 types with resistivities ρ_0 (at $T_0 = 293\ K$) equal to $0.50\ \Omega \cdot cm$, $1\ \Omega \cdot cm$, $10\ \Omega \cdot cm$ respectively. Unification of the sensor design with the input mechanical quantities will be related to changing the slope of the conversion characteristic by selecting the thickness of the elastic element. An important condition is the independence of the circuit parameters from the thickness H_{ee}. From the graph in Fig. 3.6, which shows the experimental dependence of the change in the input resistance R_{in} on the calculated parameter $\frac{H_{ee}}{a}$, it can be seen that this condition will hold at $\frac{H_{ee}}{a} \geqslant 0.3$. The dependence of the parameter Λ on the resistivity ρ_{ee} was determined by measuring test samples of thickness $H_{EE} = 1 \cdot 10^{-2} cm$. The change in Λ values for $\rho_{ee} = (0.5 \div 10)\ \Omega \cdot cm$ was within the measurement error. For samples in which piezoresistive channels were formed by boron ion implantation with a doping dose of $2 \cdot 10^{15} cm^{-2}$, $\Lambda = (9.1 \pm 0.5) \cdot 10^{-3} cm$.

3. Conclusions

1. The topological structure of the bridge circuit is chosen, where equal square contact areas of size b with centers in the vertices of the square of size a are connected to each other by four single-band piezoresistive channels of width d of longitudinal and transverse piezoresistors; such a scheme will allow:
- approximate to zero the magnitude and temperature variations of the normalized null output, $K_{mc0}(T) = 0$;
- reduce the total area of the insulating p-n junction to $A_{p-n} \leq 2 \cdot 10^{-4}\ cm^2$.
2. The main regularities of the influence of physical factors on the temperature dependence of the insulating properties of $p-n$ junctions at temperatures above $100^{\circ}C$ have been established. The upper value of the working temperature range T_{per} for IPT (in which the insulation of the piezoresistive channels and contact pads of the conductivity bridge circuit of type p^{+} of the elastic element is performed by the depleted charge carriers layer $p-n$-junction) is determined by the condition when the insulation resistance value $p-n$-junction decreases to the value $R_i^{p-n} = 2.5 \cdot 10^{6}$.
3. The calculated ratio is obtained and the temperature changes of the reverse current density $p^{+}-n$-transition for IPT with resistivities EE from $0.5\ \Omega \cdot cm$ to $20\ \Omega \cdot cm$ are calculated.
4. For ITPs with specific resistances of the elastic element $\rho_{ee} \leqslant 10\ \Omega \cdot cm$ and the area of the insulating p-n junction $A_{p-n} \leqslant 1.28 \cdot 10^{-4}\ cm^2$ the calculated upper limit of the operating temperature range is determined by the values $T_{per} \geqslant 210^{\circ}C$. The discrepancy between the experimentally obtained values of T_{per} and the calculated values was not greater than $15\ \%$.
5. The relations are obtained to calculate the parameters of a strain IPT with distributed parameters (in which the piezoresistive channels and contact areas of the bridge circuit are doped with an impurity that increases the concentration of the majority charge carriers of elastic elements of silicon p type with a resistivity of $20\ \Omega \cdot cm$ to $0.5\ \Omega \cdot cm$) defining the upper limit of the operating temperature range from $+150^{\circ}C$ to $300^{\circ}C$. For a force sensor with an elastic beam element, where the design parameter $\frac{H_{EE}}{a} \geqslant 0.3$, the values of the Λ parameter characterizing the redistribution of charge carrier current in the channels and volume of the elastic element were experimentally measured. The changes in the values of the parameters Λ for IPT with resistances of $0.50\ \Omega \cdot cm$, $1\ \Omega \cdot cm$, $10\ \Omega \cdot cm$ were within the measurement error. For IPT where EE were formed by implantation of boron ions with a doping dose of $2 \cdot 10^{15}\ cm^{-2}$ the parameter Λ is $(9.1 \pm 0.5) \cdot 10^{-3}$ cm.

References

1. Tikhomirov, M. Y. (1984). Issledovanie kharakteristik izmeritel'noi skhemy kremnievogo integral'nogo preobrazovatelya mekhanIcheskoi velichiny pri temperature vyshe +100℃ [Study of the characteristics of the measuring circuit of the silicon integrated mechanical magnitude transducer at temperatures above +100℃]. *Ehlektronika i Schetno-Reshayushchaya Tekhnika v Lesnoi i Derevoobrabatyvayushchei Promyshlennosti: Sbornik Nauchnykh Trudov MLTI.*, 158(In Russian).
↩
2. Kanischeva G.A., Kilmetov R.S., Kobyakova L.P., & et al. (1978). Poluchenie vypuklykh i vognutykh ploskostei anizotropnym travleniem Si (100). [Obtaining convex and concave planes by anisotropic etching of Si (100).]. *Ehlektronnaya Tekhnika. [Electronic Engineering.] (In Russian)*, *Seriya 3*(5), 77–81.
↩
3. Bogatov, P. N., Borschev, V. N., Spalek, Y. M., & Tikhomirov, M. Y. (1976). Kremnievyi chuvstvitel'nyi ehlement dlya datchikov sil, uskorenii, vibratsii.[The silicon sensing element for sensors of forces, accelerations, vibrations]. *Tekhnologiya. Tekhnologiya Priborostroeniya: Nauch.-Tekhn.Sb. TSNTI "Poisk" (In Russian)*, 14(2), 17–27.
↩
4. *GOST 15077-78 Datchiki siloizmeritel'nye tenzorezistornye GSP. Obshchie tekhnicheskie usloviya. [Strain gauges strain gauge GSP. General specifications]*. (1978). https://files.stroyinf.ru/Data2/1/4293776/4293776163.pdf
↩
5. Stepanenko, I. P. (1980). *Osnovy mikroehlektroniki [Fundamentals of microelectronics]: Vol. (In Russian)*. Sovetskoe radio.
↩
6. Kamke, E. (1977). *Differentialgleichungen Lösungsmethoden und Lösungen*. Vieweg+Teubner Verlag. https://doi.org/10.1007/978-3-663-05925-7
↩
7. *GOST 216-16-76. Tenzorezistory. Obshchie tekhnicheskie usloviya. [State Standard 216-16-76. Strain gauges. General specifications]*. (1976). https://docs.cntd.ru/document/1200023567
↩
8. Osipovich, L. A. (1979). *Datchiki fizicheskikh velichin. [Sensors of physical quantities.]: Vol. (In Russian)*. Mashinostroenie.

↩
9. Kulikovskii, K. L., & Kuper, V. Y. (1986). *Metody i sredstva izmereniya. [Methods and means of measurement.]*: *Vol. (In Russian)*. Ehnergoatomizdat.
↩